NUMERICAL ANALYSIS OF A STEADY FLOW IN A NON-UNIFORM CAPILLARY

by

Ya-Ping LI[a,b], Li-Li WANG[b], and Jie FAN[a,b*]

[a] Key Laboratory of Advanced Textile Composites, Ministry of Education of China, Tiangong University, Tianjin, China
[b] School of Textile Science and Engineering, Tiangong University, Tianjin, China

Original scientific paper
https://doi.org/10.2298/TSCI2004385L

Fluids in porous media driven by the capillary force are greatly affected by capillary's geometrical structure. The steady flow in a non-uniform capillary is numerically analyzed by the finite element method. With the given initial and boundary conditions, the flow velocity distribution with different geometrical parameters is obtained, and the result is in a good agreement with the experimental data.

Key words: *fluid-flow property, non-uniform capillary, numerical simulation, geometrical parameter*

Introduction

Fluid-flow management in porous media has significant applications in water collection [1, 2], separators for batteries [3, 4], microfluids [5-7], capillary vibration [8], functional textiles [9, 10], and solar steam generation [11, 12]. In most situations, porous media have an irregular complex inner structure. With the development of science, fluid-flow in non-uniform capillaries of a porous medium attracted more and more interest of researchers. Erickson *et al.* [13] found theoretically that the non-uniform cross-sectional capillaries exhibited remarkably slower wetting behavior than straight capillaries. Young *et al.* [14] obtained the same result by constructing a simple formulation based on analysis of the Lucas-Washburn equation for simulation of the interface progression in a non-uniform capillary. Liou *et al.* [15] further developed the non-uniform cross-sectional capillary flow model based on the Navier-Stokes equations, incorporating inertial and viscous terms, which are applicable to different wall variations. Shou *et al.* [16] investigated the geometry-induced fluid-flow in multi-section porous paper layers, and suggested that the two-section structures with a negative gradient of radius against the absorption direction have faster absorption rates than those with uniform radius. Recently, we established the lotus-rhizome-node-like non-uniform capillary model which illustrated the relationship between the wicking behavior of the non-uniform capillary and its geometrical structure parameters [17]. Yang *et al.* [18] used the spinneret's geometrical structure to fabricate shaped fibers, and a non-uniform capillary can be formed when the shaped fibers are combined together. He and Ji [19, 20], He [21], and Ain and He [22] suggested a Taylor series method and a two-scale thermodynamics to deal with non-linear problems using two scales. Fan *et al.* [23] explained the cell orientation on non-uniform capillaries that con-

* Corresponding author, e-mail: fanjie@tjpu.edu.cn

structed by nanofibers of different orientation by the geometric potential theory. All of the investigations suggest that the irregular fluid transport path has a substantial influence on the fluid-flow performance, and the fluid transport process can be controlled by adjusting the structure of the porous media.

In this paper, the steady flow behavior in the non-uniform capillaries will be numerically investigated based on the finite element method. The influence of the geometrical parameters of the non-uniform capillary on the capillary flow velocity is analyzed.

The lotus-rhizome-node-like non-uniform capillary

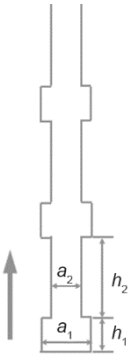

Figure 1. Schematic diagram of non-uniform capillary

For the capillary flow in a porous medium, a liquid will spontaneously find a continuous channel driven by the capillary force, forming a non-uniform capillary in porous media. For a homogenously porous media, such as sponge, yarns, the non-uniform capillary can be simplified as a capillary composed of a series of alternatively arranged converging and diverging sections, shown in fig. 1. The width and the height of the diverging section are a_1 and h_1, and the width and the height of the converging section are a_2 and h_2, respectively. The n is defined as the length ratio between the converging section and diverging section, and m is defined as the width ratio between the converging section and diverging section, respectively; let $n > 1$ and $0 < m < 1$.

To investigate the effect of the different geometrical parameters of the capillary on the steady-state fluid-flow performance. We establish three groups of non-uniform capillaries, each group of capillaries has the same volume, shown in tabs. 1-3.

Table 1. Non-uniform capillaries with different alternate frequency between the converging and diverging sections (n = 2, m = 0.3)

Sample	Number of sections	Type	Height [μm]	Width [μm]
a	16	Diverging	150	60
		Converging	300	18
b	32	Diverging	75	60
		Converging	150	18

Table 2. Non-uniform capillary with different width ratio between the converging and diverging section

Sample	Height and width ratio	Type	Height [μm]	Width [μm]
b	n = 2, m = 0.3	Diverging	75	60
		Converging	150	18
c	n = 2, m = 0.5	Diverging	75	48
		Converging	150	24

Table 3. Non-uniform capillary with different width ratio between the converging and diverging section

Sample	Height and width ratio	Type	Height [μm]	Width [μm]
d	$n = 2$, $m = 0.4$	Diverging	100	60
		Converging	200	24
e	$n = 5$, $m = 0.4$	Diverging	50	72
		Converging	250	28.8

Finite element model

In order to avoid complex calculation, we choose 3.5 mm non-uniform capillary model as the representative unit cell for fluid-flow simulation, as was shown in fig. 2.

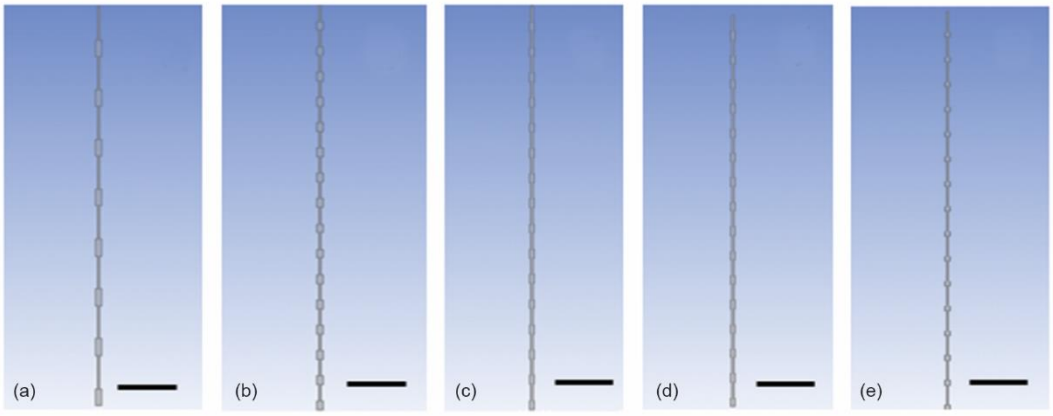

Figure 2. Physical model of non-uniform capillary with different geometrical parameters bar = 500 μm (the structural parameter of samples a-e are listed in tabs. 1-3)

The physical models of the non-uniform capillaries were then imported into ANSYS Workbench. All triangles method were used to mesh the unit cells. The optimal mesh density was obtained after verification that the refinement does not affect the result, and the number of nodes and elements are listed in tab. 4. Figure 3 shows the partial enlarged detail of each non-uniform capillary.

Table 4. The number of nodes and elements of the non-uniform capillaries

Sample	Nodes	Elements
a	26707	49088
b	24763	44864
c	27220	50091
d	23854	43271
e	23017	41560

The 1-D fluid-flow in non-uniform capillaries is driven by the capillary force, which can be express by Young-Laplace law:

$$P_c = -\frac{2\gamma\cos\theta}{a} \tag{1}$$

where γ [Nm^{-1}] is the surface tension of liquid, a [m] – the width of capillary, θ [°] – the contact angle.

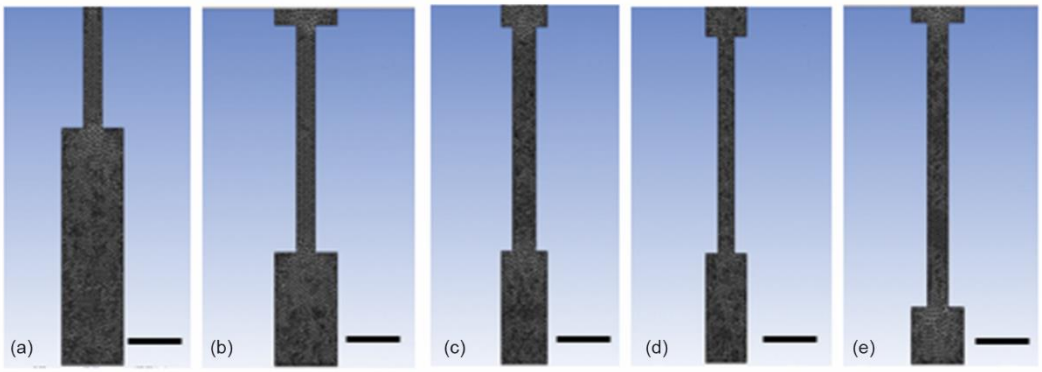

Figure 3. Mesh generation of non-uniform capillaries with different geometrical parameters (part map) bar = 100 μm (the structural parameter of samples a-e are listed in tabs. 1-3)

For the case that water flow in the non-uniform capillary composed by polypropylene fiber, the water surface tension is $\gamma = 7.2\cdot10^{-2}$ N/m, the contact angle between polypropylene and water is $\theta = 66.5°$. Setting the diverging section as the liquid entrance of the non-uniform capillaries. The width of liquid entrance a for each non-uniform capillary is listed in tab. 5. Considering that the atmosphere pressure at the entrance and outlet is offset. The inlet pressure of non-uniform capillaries is set as the capillary force of the diverging section of each capillary. The inlet pressure of each capillary was calculated according to eq. (1) and listed in tab. 5. The outlet pressure are set as zero.

Table 5. Inlet/outlet pressure and the entrance dimension of the capillaries

Sample	Entrance pressure	Outlet pressure	a [m]
a	960 Pa	0	$6\cdot10^{-5}$ m
b	960 Pa	0	$6\cdot10^{-5}$ m
c	1200 Pa	0	$4.8\cdot10^{-5}$ m
d	960 Pa	0	$6\cdot10^{-5}$ m
e	800 Pa	0	$7.2\cdot10^{-5}$ m

When fluid-flows in thin capillary, the water flow velocity is relatively low. Thus, the water wicking phenomenon in thin non-uniform capillary corresponds to a small Reynolds number value. As a result, we choose the Phan-Thien-Tanner model as the physical model.

Numerical results and analysis

The steady-state fluid-flow velocity distribution and the steady-state fluid-flow velocity on the axis of the converging and diverging sections are shown in fig. 4, and the fluid-flow velocity on the axis of the converging and diverging section is listed in tab. 6.

Table 6. Maximum and minimum fluid-flow velocity on axis of the converging and diverging section

Sample	Velocity on axis of converging section [ms^{-1}]	Velocity on axis of diverging section [ms^{-1}]
a	$4.9\cdot10^{-3}$	$15.8\cdot10^{-3}$
b	$5\cdot10^{-3}$	$15.2\cdot10^{-3}$
c	$16.25\cdot10^{-3}$	$32\cdot10^{-3}$
d	$6.8\cdot10^{-3}$	$19.1\cdot10^{-3}$
e	$11\cdot10^{-3}$	$20.6\cdot10^{-3}$

Figures 4(a) and 4(b) suggest that when capillaries have the same height and width ratio between the diverging and converging sections but different alternate frequencies, the capillary with low alternate frequencies between the diverging and converging sections has a relatively faster flow velocity with a maximum flow velocity of $15.8\cdot10^{-3}$ m/s, fig. 4(a) on the diverging section, while the capillary with high alternate frequencies between the diverging and converging sections has a relatively slower flow velocity with a maximum flow velocity of $15.2\cdot10^{-3}$ m/s, fig. 4(a) on the diverging section. The high alternate frequency between the diverging and converging sections increases the unevenness of the capillary. Thus, the capillary with low alternate frequency of segments has a faster flow velocity.

It can be seen from figs. 4(b) and 4(c) that when the height ratio between the converging and diverging sections of capillaries is same, the capillary with a larger width ration between the converging and diverging section exhibits a distinct faster flow velocity of $32\cdot10^{-3}$ m/s, fig. 4(c) on the diverging section, which is over two times of that, $15.2\cdot10^{-3}$ m/s, fig. 4(b), on the capillary with a smaller width ration between the converging and diverging section. That is because when the width ration between the converging and diverging section increases, the width different between the converging and diverging section decreases, thus, the evenness of capillary increases, and the capillary with larger width ratio between the converging and diverging section has a faster flow velocity.

Comparing figs. 4(d) and 4(e), we found that when the width ratio between the converging and diverging sections of capillaries is same, the capillary with larger height ratio between the converging and diverging sections has a relatively faster flow velocity of $20.6\cdot10^{-3}$ m/s on the diverging section and $11\cdot10^{-3}$ m/s on the converging section, fig. 4(e), while flow velocity of the capillary with smaller height ratio between the converging and diverging sections has a slower flow velocity of $19.1\cdot10^{-3}$ m/s on axis of the diverging section, and $6.8\cdot10^{-3}$ m/s on the converging section, fig. (d). That is due to the short converging section of the capillary with larger height ratio between the converging and diverging sections has a relatively larger effective diameter comparing with that of the capillary with small height ratio between the converging and diverging sections. As a result, the capillary with larger height ratio between the converging and diverging sections has a relatively faster flow velocity.

The previous numerical results were in consistent with the analytical solution of the normalized total flow time equation previously reported in reference [17].

Conclusions

In this study, the steady-state fluid-flow in non-uniform capillary are numerically investigated using the finite element method with Phan-Thien-Tanner model. The fluid-flow

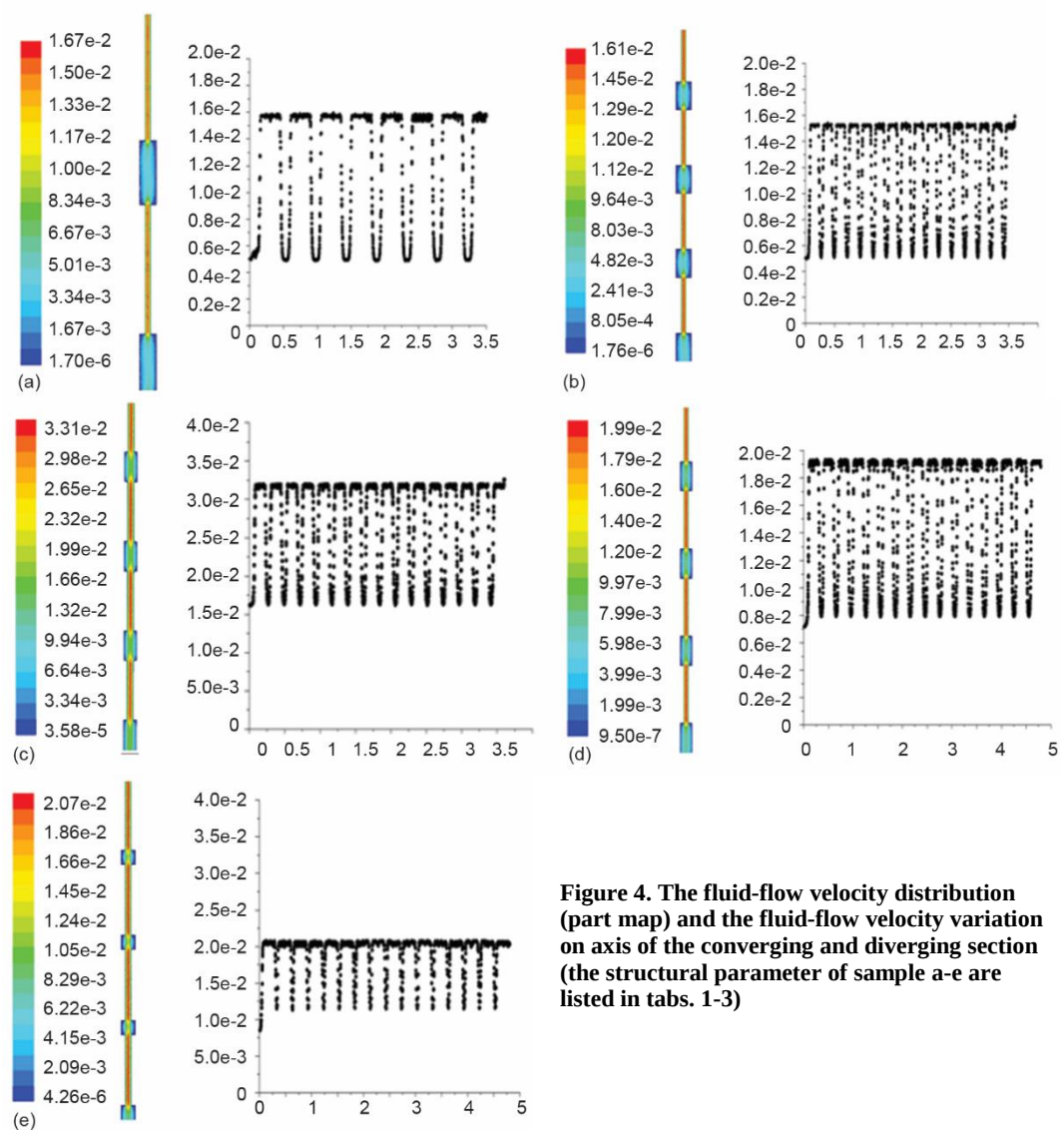

Figure 4. The fluid-flow velocity distribution (part map) and the fluid-flow velocity variation on axis of the converging and diverging section (the structural parameter of sample a-e are listed in tabs. 1-3)

velocity profile suggests that the geometrical structure of non-uniform capillary has a great effect on the wicking behavior of liquid. For non-uniform capillaries with same volume, the non-uniform capillary which has a low alternative frequency between the diverging and converging section, larger width ratio between the converging section and diverging section, and larger height ratio between the converging and diverging sections shows a relatively faster fluid-flow velocity due to the relatively more evenness of the capillary. The results obtained are in agreement with the analytical solution we previously reported.

Acknowledgment

This work was supported by the National Key R&D Program of China (Grant Number 2017YFB0309100).

References

[1] Chen, H., *et al.*, Ultrafast Water Harvesting and Transportin Hier Archical Microchannels, Nature Materials, *17* (2018), 10, pp. 935-942
[2] Song, Y.-Y., *et al.*, Bioinspired Fabrication of One Dimensional Graphene Fiber with Collection of Droplets Application, Scientific Reports, *7* (2017), 1, pp. 12056-12056
[3] Liu, X., *et al.*, Electrospun PU@GO Separators for Advanced Lithium Ion Batteries, *Journal of Membrane Science, 555* (2018), June, pp. 1-6
[4] Zhu, P., *et al.*, A Novel Bi-Functional Double-Layer rGO-PVDF/PVDF Composite Nanofiber Membrane Separator with Enhanced Thermal Stability and Effective Polysulfide Inhibition for High-Performance Lithium-Sulfur Batteries, *Journal of Materials Chemistry A, 5* (2017), 29, pp. 15096-15104
[5] Shou, D., Fan, J., Design of Nanofibrous and Microfibrous Channels for Fast Capillary Flow, Langmuir, *34* (2018), 4, pp. 1235-1241
[6] Shang, L., *et al.*, Bio-Inspired Stimuli-Responsive Graphene Oxide Fibers from Microfluidics, *Journal of Materials Chemistry A, 5* (2017), 29, pp. 15026-15030
[7] Shou, D., Fan, J., An All Hydrophilic Fluid Diode for Unidirectional Flow in Porous Systems, *Advanced Functional Materials, 28* (2018), 36, ID 1800269
[8] Jin, X., *et al.*, Low Frequency of a Deforming Capillary Vibration: Part 1 Mathematical Model, *Journal of Low Frequency Noise, Vibration and Active Control, 38* (2019), 3-4, pp. 1676-1680,
[9] Ge, J., *et al.*, Biomimetic and Superwettable Nanofibrous Skins for Highly Efficient Separation of Oil-in-Water Emulsions, *Advanced Functional Materials, 28* (2018), 10, ID 1705051
[10] Fan, J., *et al.*, Influence of Hierarchic Structure on the Moisture Permeability of Biomimic Woven Fabric Using Fractal Derivative Method, *Advances in Mathematical Physics, 2015* (2015), ID 817437
[11] Chen, C., *et al.*, Highly Flexible and Efficient Solar Steam Generation Device, *Advanced Materials, 29* (2017), 30, ID 1701756
[12] Li, T., *et al.*, Scalable and Highly Efficient Mesoporous Wood-Based Solar Steam Generation Device: Localized Heat, Rapid Water Transport, *Advanced Functional Materials, 28* (2018), ID 1707134
[13] Erickson, D., *et al.*, Numerical Simulations of Capillary-Driven Flows in Nonuniform Cross-Sectional Capillaries, *Journal of Colloid and Interface Science, 250* (2002), 2, pp. 422-430
[14] Young, W., Analysis of Capillary Flows in Non-Uniform Cross-Sectional Capillaries, *Colloids And Surfaces A: Physicochemical and Engineering Aspects, 234* (2004), 1-3, pp. 123-128
[15] Liou, W. W., *et al.*, Analytical Modeling of Capillary Flow in Tubes of Nonuniform Cross Section, *Journal of Colloid and Interface Science, 333* (2009), 1, pp. 389-399
[16] Shou, D., *et al.*, Geometry-Induced Asymmetric Capillary Flow, *Langmuir, 30* (2014), 19, pp. 5448-5454
[17] Fan, J., *et al.*, Liquid Transport in Non-Uniform Capillary Fibrous Media, *Textile Research Journal, 89* (2019), 9, pp. 1684-1698
[18] Yang, Z. P., *et al.*,On the Cross-Section of Shaped Fibers in the Dry Spinning Process: Physical Explanation by the Geometric Potential Theory, *Results in Physics, 14* (2019), ID 102347
[19] He, J. H. Ji, F. Y., Taylor Series Solution for Lane-Emden Equation, *Journal of Mathematical Chemistry, 57* (2019), 8, pp. 1932-1934
[20] He, J. H., Ji, F. Y., Two-Scale Mathematics and Fractional Calculus for Thermodynamics, *Thermal Science, 23* (2019), 4, pp. 2131-2133
He, J. H., The Simplest Approach to Non-Linear Oscillators, *Results in Physics, 15* (2019), ID 102546
[21] Ain, Q. T., He, J. H., On Two-Scale Dimension and Its Applications, *Thermal Science, 23* (2019), 3B, pp. 1707-1712
[22] Fan, J., *et al.* Explanation of the Cell Orientation in a Nanofiber Membrane by the Geometric Potential Theory, *Results in Physics, 15* (2019), Dec., ID 102537

Paper submitted: March 6, 2019
Paper revised: September 4, 2019
Paper accepted: August 12, 2019